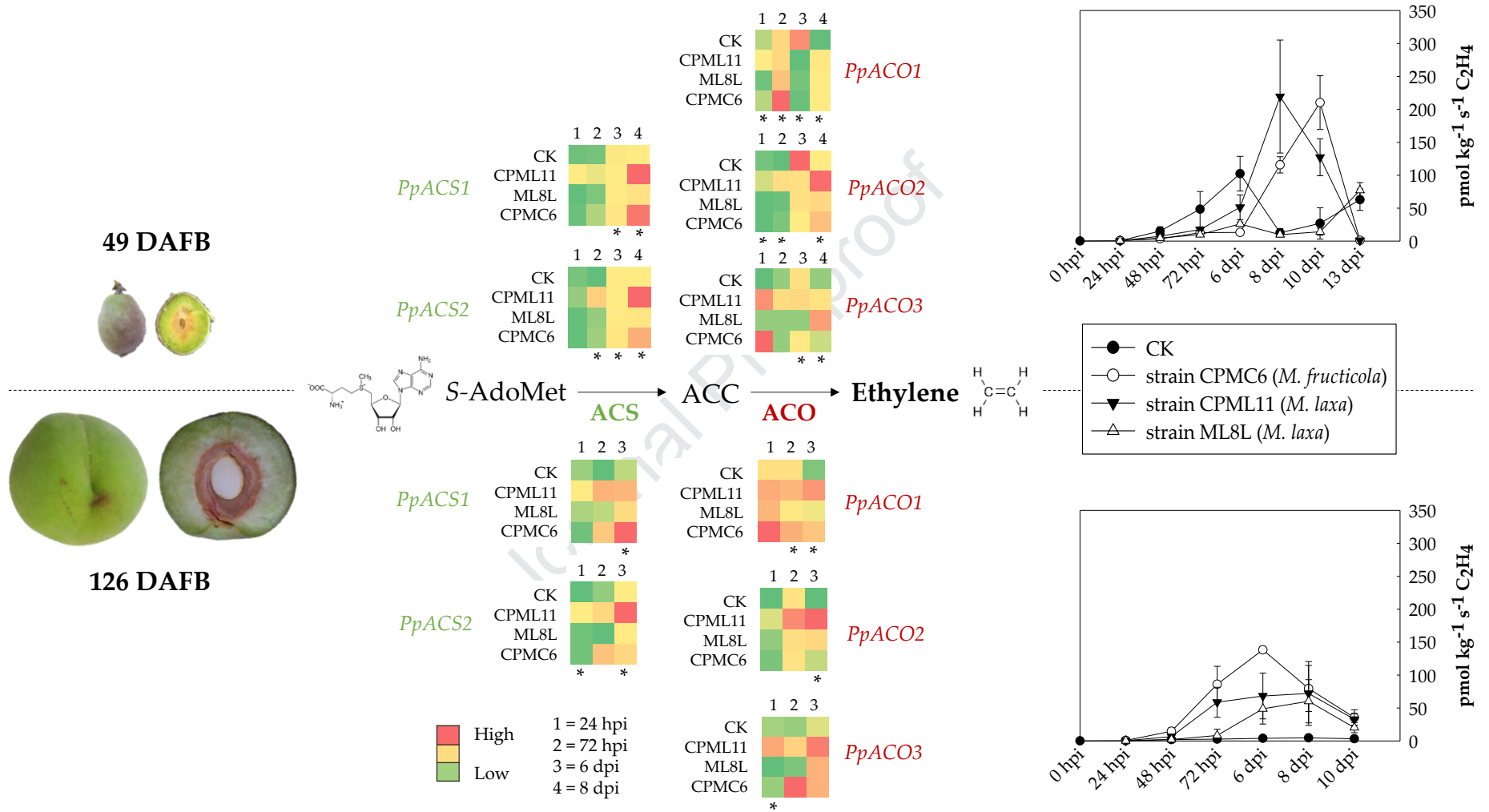




**This document is a postprint version of an article published in Plant Physiology and Biochemistry © Elsevier after peer review. To access the final edited and published work see <https://doi.org/10.1016/j.plaphy.2019.09.048>**

**Document downloaded from:**





1 **Double-sided battle: the role of ethylene during *Monilinia* spp. infection in peach**  
2 **at different phenological stages**

3

4 Núria Baró-Montel, Núria Vall-llaura, Jordi Giné-Bordonaba, Josep Usall, Sandra  
5 Serrano-Prieto, Neus Teixidó and Rosario Torres

6 *IRTA, XaRTA-Postharvest, Edifici Fruitcentre, Parc Científic i Tecnològic*  
7 *Agroalimentari de Lleida, Parc de Gardeny, 25003 Lleida, Catalonia, Spain.*

8

9 \*Corresponding Author: Rosario Torres

10 Phone: 973 00 34 30

11 E-mail: [rosario.torres@irta.cat](mailto:rosario.torres@irta.cat)

12

13

14

15

16

17

18

19 **Abstract**

20 Controversy exists on whether ethylene is involved in determining fruit resistance or  
21 susceptibility against biotic stress. In this work, the hypothesis that ethylene  
22 biosynthesis in peaches at different phenological stages may be modulated by *Monilinia*  
23 spp. was tested. To achieve this, at 49 and 126 d after full bloom (DAFB), ethylene  
24 biosynthesis of healthy and infected ‘Merryl O’Henry’ peaches with three strains of  
25 *Monilinia* spp. (*M. fructicola* (CPMC6) and *M. laxa* (CPML11 and ML8L) that differ in  
26 terms of aggressiveness) was analysed at the biochemical and molecular level along the  
27 course of infection in fruit stored at 20 °C. At 49 DAFB, results evidenced that infected  
28 fruit showed inhibition of ethylene production in comparison with non-inoculated fruit,  
29 suggesting that the three *Monilinia* strains were somehow suppressing ethylene  
30 biosynthesis to modify fruit defences to successfully infect the host. On the contrary, at  
31 126 DAFB ethylene production increased concomitantly with brown rot spread, and  
32 values for non-inoculated fruit were almost undetectable throughout storage at 20 °C.  
33 The expression of several target genes involved in the ethylene biosynthetic pathway  
34 confirmed that they were differentially expressed upon *Monilinia* infection, pointing to  
35 a strain-dependent regulation. Notably, *Prunus persica* 1-aminocyclopropane-1-  
36 carboxylic acid (ACC) synthase (ACS) (*PpACS*) family was the most over-expressed  
37 over time, demonstrating a positive ethylene regulation, especially at 126 DAFB. At  
38 this phenological stage it was demonstrated the ability of *Monilinia* spp. to alter  
39 ethylene biosynthesis through *PpACSI* and benefit from the consequences of an  
40 ethylene burst likely on cell wall softening. Overall, our results put forward that  
41 infection not only among different strains but also at each stage is achieved by different  
42 mechanisms, with ethylene being a key factor in determining peach resistance or  
43 susceptibility to brown rot.

44 **Keywords:** 1-aminocyclopropane-1-carboxylic acid (ACC), ACC oxidase (ACO), ACC  
45 synthase (ACS), brown rot, gene expression analysis, host-pathogen interaction, *Prunus*  
46 *persica*.

47

## 48 **1. Introduction**

49 Brown rot caused by *Monilinia* spp. have attained great importance worldwide as the  
50 pathogen have been disseminated and is responsible of enormous economic losses in  
51 postharvest of stone fruit. Additionally, the management of this disease is facing  
52 obstacles due to the emerging fungicide resistance and the growing public concerns over  
53 fungicide usage. In this context, the irruption of “omics” has prompted a renewed  
54 interest in molecular genetic approaches to study fruit-pathogen interactions from a  
55 global point of view which, in turn, resulted in important advances towards searching  
56 new control strategies (Tian et al., 2016). In particular, for brown rot, both the host  
57 (peach) (Verde et al., 2013) and the pathogen (*Monilinia* spp.) (Landi et al., 2018;  
58 Naranjo-Ortíz et al., 2018; Rivera et al., 2018) genomes are currently available. As a  
59 result, the process of understanding the pathogen’s virulence factors and the fruit  
60 resistance/susceptibility mechanisms is now becoming more feasible.

61 Using functional genomics, many research groups are highlighting the potential that  
62 studying the host immune system can have in disease protection (reviewed in Pétriacq et  
63 al., 2018). Plants are in continuous exposure to various forms of biotic stresses such as  
64 insects and pathogens. In response, they express numerous constitutive and induced  
65 defence mechanisms (reviewed in Pandey et al., 2016). Once constitutive mechanisms  
66 (i.e., structural or physical barriers) have been trespassed by the pathogen, inducible

67 defence mechanisms become responsible for halting pathogen progress. These  
68 mechanisms involve responses that rely on a network of cross-communicating signalling  
69 pathways of which salicylic acid, jasmonic acid and ethylene are the principal mediators  
70 in plants (De Vos et al., 2005). Besides, jasmonic acid and ethylene are considered to  
71 play pivotal roles in regulating the plant response towards necrotrophic fungal infection  
72 (Glazebrook, 2005; Pandey et al., 2016). Specifically, for *M. laxa* further evidence was  
73 provided from the dramatic changes in the expression of phenylpropanoid and  
74 jasmonate-related genes obtained by microarray analysis of susceptible (two weeks  
75 before pit hardening) and resistant (pit hardening) phases (Guidarelli et al., 2014). Both  
76 the phenylpropanoid and jasmonate pathways are ethylene-dependent (Broekgaarden et  
77 al., 2015; Ecker and Davis, 1987; Wang et al., 2002). Ethylene is a simple gaseous  
78 hydrocarbon first discovered for its role in fruit maturation, senescence, germination and  
79 flowering (Bleecker and Kende, 2000; Payton et al., 1996), but it was later shown to also  
80 function as a modulator of the plant immune signalling network (reviewed in van Loon  
81 et al., 2006).

82 The biosynthesis of ethylene consists of two enzymatic steps: a first level of regulation  
83 occurs by the action of the enzyme 1-aminocyclopropane-1-carboxylic acid (ACC)  
84 synthase (ACS), followed by the oxidative cleavage of ACC by ACC oxidase (ACO)  
85 forming ethylene (Wang et al., 2002). In most instances, ACS may act as the rate-  
86 limiting step in ethylene biosynthesis, however, in conditions of high ethylene  
87 production, such as in ripening fruit, ACO is often the limiting factor (Argueso et al.,  
88 2007). Both ACS and ACO are encoded by multigene families, which are differentially  
89 expressed during fruit development and ripening (Wang et al., 2002). To date, many  
90 studies have focused on ethylene biosynthesis in peach, gaining insight into the  
91 regulation of peach ripening and the elements related to ethylene signal transduction

92 (Basset et al., 2002; Hayama et al., 2006; Rasori et al., 2002; Tadiello et al., 2016; Wang  
93 et al., 2017). However, no studies have tried to explore whether the different genes  
94 coding for the two enzymes involved in the conversion of *S*-adenosyl-methionine (*S*-  
95 AdoMet) to ethylene show a specific expression profile upon infection in the *Monilinia*  
96 spp.-stone fruit pathosystem. Noteworthy, studies aimed to elucidate the role of ethylene  
97 in determining the outcome of plant-pathogen interactions in other pathosystems (i.e.,  
98 *Botrytis cinerea*-tomato (Blanco-Ulate et al., 2013); *Penicillium digitatum*-citrus  
99 (Ballester et al., 2011; Marcos et al., 2005); *Penicillium* spp.-apples (Vilanova et al.,  
100 2017)), have provided evidence on the dual role that this hormone can play on the fruit-  
101 pathogen interactions. So far, a work recently conducted by Baró-Montel et al.  
102 (unpublished data), pointed out the importance of ethylene in determining the peach  
103 susceptibility to brown rot at different phenological stages, as well as the differential  
104 ability of three strains of *Monilinia* spp. to infect non-wounded peaches. Accordingly,  
105 the aim of this study was to further investigate whether peach ethylene biosynthesis, at  
106 the molecular level, was affected in response to *M. fructicola* and *M. laxa* infection at 49  
107 and 126 d after full bloom (DAFB), phenological stages with outstanding differences in  
108 terms of susceptibility to *Monilinia* infection. To achieve this, evolution of ethylene  
109 production and expression pattern of genes coding for *PpACS* and *PpACO* families were  
110 analysed over time upon infection.

## 111 **2. Material and methods**

### 112 *2.1. Plant material*

113 Experiments were conducted with ‘Merryl O’Henry’ peaches (*Prunus persica* (L.) Batch)  
114 obtained from an organic orchard located in Vilanova de Segrià (Lleida, Catalonia, NE  
115 Spain). Fruit free of physical injuries and rot were picked at 49 and 126 DAFB, being full

116 bloom the stage when at least 50 % of flowers were opened, and framed in the BBCH scale  
117 (Meier et al., 1994) as follows: 49 (BBCH = 72) and 126 (BBCH = 81). After each  
118 harvest, peaches were immediately transported to IRTA facilities under acclimatised  
119 conditions (20 °C).

## 120 2.2. Pathogen and inoculum preparation

121 In this study three single-spore strains of *Monilinia* spp. were used: *M. fructicola* (CPMC6)  
122 and *M. laxa* (CPML11 and ML8L), being different in terms of aggressiveness and coming  
123 from different sources. The strain CPML11 belong to the collection of the Postharvest  
124 Pathology group of IRTA (Lleida, Catalonia, Spain). CPML11 was isolated from an  
125 infected peach fruit from a commercial orchard in Sudanel (Lleida, Spain) in 2009, and  
126 identified by the Department of Plant Protection, INIA (Madrid, Spain). The strains  
127 CPMC6 and ML8L were isolated from a latent infection of a peach fruit from a commercial  
128 orchard in Alfarràs (Lleida, Spain) in 2010, and from a mummified ‘Sungold’ plum fruit  
129 from a commercial orchard in Lagunilla (Salamanca, Spain) in 2015, respectively, and  
130 are deposited in the Spanish Culture Type Collection (CECT 21105 and CECT 21100,  
131 respectively). All strains were maintained in 20 % glycerol (w/v) at -80 °C for long-term  
132 storage and subcultured periodically on Petri dishes containing potato dextrose agar (PDA;  
133 Biokar Diagnostics, 39 g L<sup>-1</sup>) supplemented with 25 % tomato pulp and incubated under 12-  
134 h photoperiod at 25 °C / 18 °C for 7 d.

135 Conidial suspensions of the fungal cultures were prepared by adding 10 mL of sterile water  
136 with 0.01 % Tween-80 (w/v) as a wetting agent over the surface of 7-day-old cultures  
137 grown on PDA supplemented with 25 % of tomato pulp and scraping the surface of the agar  
138 with a sterile glass rod. The inoculum was filtered through two layers of sterile cheesecloth



139 to minimize the presence of mycelial fragments. Then, conidia were counted in a  
140 haemocytometer and diluted to the desired concentration ( $10^5$  conidia  $\text{mL}^{-1}$ ).

### 141 *2.3.Fruit inoculation and experimental design*

142 ‘Merryl O’Henry’ peaches were disinfected with 0.5 % (v/v) sodium hypochlorite  
143 (NaClO) for 180 s and rinsed five times with tap water. Once dried, fruit were separated  
144 into four sets according to the treatment being applied. Then, non-wounded fruit were  
145 immersed for 60 s in a tank of running tap water containing a concentration of  $10^5$  conidia  
146  $\text{mL}^{-1}$  of strain CPMC6, CPML11 or ML8L. The remaining set was immersed in a tank  
147 containing only water, and thus serve as a control (CK). After that, fruit were placed on  
148 plastic holders in simple, lidded, storage boxes containing water at the bottom (not in  
149 contact with the sample) and separated into three different batches depending on whether  
150 they were used for: i) assessment of brown rot susceptibility, ii) determination of ethylene  
151 production and respiration rate, and iii) gene expression analysis. All the fruit was incubated  
152 in a chamber for a maximum of 14 d at 20 °C.

#### 153 *2.3.1. Assessment of brown rot susceptibility*

154 Fruit were inspected daily to know when disease symptoms initiated, but the number of  
155 brown rot infected fruit was recorded only after 7 and 14 d of incubation. Experiments were  
156 conducted with 4 replicates of 10 fruit each, thereby assessing 40 fruit per each  
157 phenological growth stage and pathogen.

#### 158 *2.3.2. Determination of ethylene production and respiration rate*

159 Fruit ethylene production was measured at 24 h, 48 h, 72 h, 6 d, 8 d, 10 d and 13 d post-  
160 inoculation. At each sampling point, fruit were placed in 2 L sealed flasks, in an

161 acclimatised chamber at 20 °C, equipped with a silicon septum for sampling the gas of  
162 the headspace after 2 h incubation. For the analysis of ethylene production, gas samples  
163 (1 mL) were taken using a syringe and injected into a gas chromatograph (Agilent  
164 Technologies 6890, Wilmington, Germany) fitted with a FID detector and an alumina  
165 column F1 80/100 (2 m × 1/8 × 2.1, Tecknokroma, Barcelona, Spain) using the  
166 methodology described elsewhere (Giné-Bordonaba et al., 2017). Results were  
167 expressed on a standard weight basis ( $\text{pmol kg}^{-1} \text{s}^{-1} \text{C}_2\text{H}_4$ ). Experiments were conducted  
168 with 4 replicates of 5 fruit each, thereby assessing 20 fruit per each phenological growth  
169 stage and pathogen.

170 Fruit respiration was determined from the same flasks used for ethylene measurements.  
171 After 2 h incubation at 20 °C, the headspace gas composition was quantified using a  
172 handheld gas analyser (CheckPoint O<sub>2</sub>/CO<sub>2</sub>, PBI Dansensor, Ringsted, Denmark).  
173 Results were expressed on a standard weight basis ( $\text{nmol kg}^{-1} \text{s}^{-1} \text{CO}_2$ ). The fruit  
174 respiratory quotient (RQ) was determined by the ratio of the amount of carbon dioxide  
175 produced divided by the amount of oxygen consumed after the 2 h incubation period.  
176 Experiments were conducted with 4 replicates of 5 fruit each, thereby assessing 20 fruit per  
177 each phenological growth stage and pathogen.

### 178 2.3.3. *Gene expression analysis*

179 At 24 h, 72 h, 6 d and 8 d post-inoculation, samples of peel and pulp tissue (10 mm  
180 diameter and 5 mm deep) encompassing all the surface of the fruit were collected using a  
181 cork borer and immediately frozen with liquid nitrogen. Afterwards, samples were  
182 lyophilised in a freeze-dryer (Cryodos, Telstar S.A., Terrassa, Spain) operating at 1 Pa and -  
183 50 °C for 5 d and grounded prior to being kept at -80 °C until further molecular analysis.

184 Experiments were conducted with 3 replicates of 5 fruit each, thereby assessing 15 fruit per  
185 each phenological growth stage, pathogen and sampling point.

### 186 2.3.3.1. RNA extraction

187 Total RNA corresponding to the healthy or infected fruit at each sampling point was  
188 extracted following the protocol described by Ballester et al. (2006) with some  
189 modifications. Briefly, 1 g of peach tissue (pulp and peel) was added to a preheated  
190 mixture of 5 mL phenol and 10 mL extraction buffer (200 mM Tris-HCl, pH 8.0, 400  
191 mM NaCl, 50 mM EDTA pH 8.0, 2 % *L*-lauroylsarcosine sodium salt (w/v), 1 %  
192 polyvinylpyrrolidone 40 (w/v), 1 %  $\beta$ -mercaptoethanol). The extract was incubated for  
193 15 minutes at 65 °C and cooled before 5 mL of chloroform-isoamyl alcohol (24:1, v/v)  
194 were added. The homogenate was centrifuged at 2,200 g during 20 minutes at 4 °C. The  
195 aqueous phase was recovered, re-extracted with 10 mL phenol-chloroform-isoamyl  
196 alcohol (25:24:21, v/v/v) and centrifuged at 2,200 g for 20 minutes at 4 °C. The aqueous  
197 phase was transferred to a new tub and centrifuged again at 24,600 g for 15 minutes at 4  
198 °C. The supernatant was recovered and precipitated overnight at – 20 °C by adding one  
199 third volume of 12 M lithium chloride. 1 mL of 3 M sodium acetate was added to the  
200 pellet obtained after centrifugation at 24,600 g for 45 minutes at 4 °C and centrifuged  
201 again at 13,900 g for 5 minutes at room temperature. The pellet obtained was washed in  
202 70 % ethanol and centrifuged as before. The pellet was finally dissolved in 50  $\mu$ L of  
203 water, incubated at 65 °C for 10 minutes and centrifuged at 13,900 g for 5 minutes at  
204 room temperature. The supernatant was recovered and transferred to a new tube. RNA  
205 quantity was determined spectrophotometrically using a NanoDrop 2000  
206 spectrophotometer (Thermo Scientific, DE, USA). Contaminant DNA was removed by  
207 treating RNA extracts with Turbo DNA-free DNase (Ambion, TX, USA), following the

208 manufacturer's recommendations. Both RNA integrity and the absence of DNA were  
209 assessed after electrophoresis on an agarose gel stained with GelRed™ Nucleic Acid  
210 Gel Stain (Biotium, Hayward, CA, USA). First-strand cDNA synthesis was performed  
211 on 3 µg of DNase-treated RNA using the SuperScript IV First-Strand Synthesis System  
212 (Invitrogen, Carlsbad, CA, USA).

#### 213 2.3.3.2. Primers design and validation

214 The primers used for quantitative real-time polymerase chain reaction (RT-qPCR)  
215 analysis (Table S1) were adopted from the literature (Tadiello et al., 2016). Among the  
216 members of ACS and ACO families reported in the cited study, the genes *PpACS1*,  
217 *PpACS2*, *PpACO1*, *PpACO2* and *PpACO3* were selected based on their relative  
218 expression profiles in fruit at different stages of development, specifically at 49 and 126  
219 DAFB. Genes encoding for translation elongation factor 2 (*TEF2*) and RNA polymerase  
220 II (*RPII*) were used as independent reference genes in all the experiments due to its high  
221 statistical reliability (Tong et al., 2009). Annealing temperature conditions for each pair  
222 of primers of both target and reference genes were optimised in the annealing  
223 temperature range of 58-62 °C using the Verity Thermal Cycler 96-wells Fast (Applied  
224 Biosystems, Foster City, CA). Additionally, non-amplification of the cDNA derived  
225 from the fungi was also verified. Primer efficiency was determined by the serial dilution  
226 method, using a mix of all cDNA samples as a template (Table S1).

#### 227 2.3.3.3. Relative quantification by RT-qPCR

228 RT-qPCR was performed on a 7500 Real Time PCR System (Applied Biosystems). The  
229 reaction mix consisted of KAPA SYBR® Fast qPCR Master Mix (Kapa Biosystems,  
230 Inc., Wilmington, USA), 100 nM of each primer and the amount of diluted cDNA,

231 according to standard curves. Thermal conditions applied were as follows: i) initial  
232 denaturation at 95 °C for 10 min, ii) 40 cycles of denaturation at 95 °C for 15 s, and iii)  
233 annealing/extension at 60 °C for 1 min. To determine the melting curve, a final  
234 amplification cycle at 95 °C for 15 s, 60 °C for 1 min, 95 °C for 30 s and 60 °C for 15 s  
235 was applied. In all cases, a non-template control (NTC) was included using DNase free  
236 water instead of DNA. The standard Cq method (Pfaffl, 2001) was used to calculate the  
237 relative transcript abundance of target genes relative to 0 hpi condition and normalized  
238 to the geometrical mean of both reference genes. Three technical replicates were  
239 analysed for each biological replicate for both the target and the reference genes.

#### 240 *2.4. Statistical analysis*

241 Data were collated and statistically analysed with JMP<sup>®</sup> software version 13.1.0 (SAS  
242 Institute Inc., Cary, NC, USA). Means were analysed by analysis of variance (ANOVA)  
243 of data expressed on a standard fresh weight basis. When the analysis was statistically  
244 significant, the Tukey's HSD test at the level  $p < 0.05$  was performed for comparison of  
245 means, while comparisons between phenological stages (49 vs. 126 DAFB) for each  
246 pathogen at specific time was done by least significance difference value test (LSD;  $p <$   
247 0.05) using critical values of  $t$  for two-tailed tests. Significance of correlations between  
248 traits was checked by Spearman's rank correlation.

### 249 **3. Results and discussion**

#### 250 *3.1. Effect of strain on the fruit susceptibility to brown rot*

251 The three single-spore strains of *Monilinia* spp. used in this study are phenotypically  
252 different when grown under *in vitro* conditions (Fig. 1A) (i.e., colour, concentric rings,  
253 morphology, spore density), but such differences were strongly confirmed with the two

254 *in vivo* approaches performed (Fig. 1B and C). In detail, the first visual infection  
255 symptoms at 49 DAFB were evident at 7 d post-inoculation (dpi) for CPMC6 and  
256 CPML11, and at 13 dpi for ML8L, whereas at 126 DAFB visual infection symptoms  
257 were evident much earlier, at 3 dpi for CPMC6 and CPML11, and at 5 dpi for ML8L.  
258 Moreover, such dissimilarities were not only visual, but also numerical since significant  
259 differences regarding its infection capacity at 7 dpi were recorded between strains  
260 CPMC6 (100 % incidence at 49 and 126 DAFB) and CPML11 (100 % and 90 %  
261 incidence at 49 and 126 DAFB, respectively), and ML8L (40 % and 23 % incidence at  
262 49 and 126 DAFB, respectively) (data not shown). Remarkably, although the time  
263 interval between infection inoculation and the onset of symptom from that infection  
264 (incubation period) for strains CPMC6 and CPML11 was the same, CPMC6 decay area  
265 was fully covered by spores, contrary to what was observed for CPML11 that mainly  
266 developed mycelium. Hence, it seemed that each strain had specific mechanisms to  
267 overwhelm peach defences, yet information regarding virulence factors of these strains  
268 is currently not available in the literature.

### 269 3.2. Analysis of ethylene production of 'Merryl O'Henry' peaches inoculated with 270 different strains of *Monilinia* spp.

271 The ethylene production and respiration rate were monitored in healthy and infected  
272 peaches covering the different fruit infection stages as depicted in Fig. 2. As regards to  
273 ethylene production at 49 DAFB, when the fruit showed low resistance to most  
274 *Monilinia* strains, significant differences were found at all sampling points, except at 24  
275 h post-inoculation (hpi) (Fig. 2A). From 24 hpi to 6 dpi values varied widely between  
276 infected and healthy peaches. In non-inoculated fruit, ethylene production increased  
277 constantly up to  $102 \text{ pmol kg}^{-1} \text{ s}^{-1}$  at 6 dpi and declined thereafter. To the best of our

278 knowledge no other studies have previously shown that fruit harvested at 49 DAFB is  
279 capable of showing a climacteric-like behavior in terms of ethylene production. Thus  
280 said, such climacteric-like ethylene production pattern was not translated into fruit  
281 softening or ripening as observed in fully mature fruit. Infected samples displayed a  
282 significant delay in the ethylene production if compared to the CK, and the ethylene  
283 peak, being higher than in non-inoculated fruit, was observed at 10 ( $210 \text{ pmol kg}^{-1} \text{ s}^{-1}$ )  
284 and 8 dpi ( $219 \text{ pmol kg}^{-1} \text{ s}^{-1}$ ) in fruit inoculated with strains CPMC6 and CPML11,  
285 respectively. For ML8L, values remained low and did not fluctuate until 13 dpi, when a  
286 5-fold increase ( $77 \text{ pmol kg}^{-1} \text{ s}^{-1}$ ) was observed. Thus, at early stages of infection the  
287 three strains seemed to suppress the ethylene production observed in non-inoculated  
288 fruit. Besides, in inoculated samples, ethylene starts to rise when disease symptoms  
289 started to be visible, which is likely related to senescence due to the maceration of the  
290 tissue in response to infection.

291 Unlike to what occurred at 49 DAFB, at 126 DAFB non-inoculated fruit did not exhibit  
292 a peak in ethylene production and levels were almost undetectable (between 0.20 and  
293  $4.81 \text{ pmol kg}^{-1} \text{ s}^{-1}$ ) (Fig. 2B). This data is in agreement with the results reported in the  
294 literature, and attributed to the low capability of converting ACC to ethylene in fruit  
295 harvested at earlier maturity stages (Yang and Hoffmann, 1984). In contrast, infected  
296 samples showed a progressive increase of ethylene production before peaking at 6 dpi  
297 for CPMC6 ( $138 \text{ pmol kg}^{-1} \text{ s}^{-1}$ ) and at 8 dpi for CPML11 ( $72 \text{ pmol kg}^{-1} \text{ s}^{-1}$ ) and ML8L  
298 ( $60 \text{ pmol kg}^{-1} \text{ s}^{-1}$ ) strains. Notably, the behavior of ML8L was identical to that of the  
299 control until 72 hpi, and as a result, both CPMC6 and CPML11 caused faster disease  
300 development and higher incidence than ML8L. In this phenological stage, the extent of  
301 the increased ethylene production in response to the inoculation was in parallel with the  
302 disease spread, and proportional to the incidence. For instance, peaches infected with

303 CPMC6 showed significantly higher ethylene production at all post-inoculation times,  
304 with the exception of 8 and 10 dpi, which may be in turn related to the more  
305 aggressiveness of this strain. Indeed, concomitantly with the increase in ethylene  
306 production, there were increments in the respiration patterns of ‘Merryl O’Henry’  
307 peaches infected with CPMC6 and CPML11 strains (Fig. 2D). These results would fit  
308 with those of Hall (1967), which observed an acceleration of the respiratory activity and  
309 ethylene production in peaches inoculated with *M. fructicola*. Furthermore, at this  
310 phenological stage respiration significantly correlated with ethylene production ( $R^2 =$   
311  $0.74$ ;  $p < 0.0001$ ), confirming that biotic stress stimulates the respiration rate of peaches.  
312 The relationship between increased ethylene levels and aggressiveness observed at this  
313 phenological stage may reflect either the fruit response to the infection or a greater  
314 capability of CPMC6 to alter ethylene production with the aim to infect its host. In  
315 accordance with this latter line, there are numerous examples, including insects (Zhu et  
316 al., 2018), viruses (Zhao et al., 2017) and fungi (Di et al., 2017) in which it has been  
317 described the ability of the pathogen to modulate the ethylene biosynthetic pathway in  
318 order to increase host susceptibility to their infection, but to date no other studies have  
319 tried to elucidate how ethylene biosynthesis in peach may be altered in response to  
320 *Monilinia* spp. infection.

321 Overall, this first approach at the physiological level pointed out that *Monilinia* strains  
322 might use two distinct mechanisms to infect peaches depending on the fruit maturity  
323 stage. Thus, while at 49 DAFB it seemed that the fungi tried to suppress the ethylene  
324 biosynthetic pathway with the ultimate goal of inhibiting fruit defence responses, at 126  
325 DAFB, when the fruit by itself is not capable of producing ethylene, the infected fruit  
326 displayed normal defence reactions, which included ethylene synthesis and increased  
327 respiration. To further investigate if physiological responses were correlated at the



328 molecular level, and also to check if the different strains of *Monilinia* were able to  
329 differentially regulate or alter the ethylene biosynthetic pathway, transcriptional  
330 responses of some *PpACO* and *PpACS* of both healthy and infected samples were  
331 analysed by qRT-PCR.

332 *3.3. Gene expression analysis of 'Merryl O'Henry' peaches inoculated with different*  
333 *strains of Monilinia spp.*

334 In detail, 8 genes encoding *ACS* and 5 genes encoding *ACO* have been described  
335 (Mathooko et al., 2001; Ruperti et al., 2001), and reported to be differentially expressed  
336 during both fruit development and ripening (Tadiello et al., 2016). However, the study  
337 presented herein was only focused on 2 genes encoding *ACS*s (*PpACS1* and *PpACS2*),  
338 and 3 genes encoding *ACOs* (*PpACO1*, *PpACO2* and *PpACO3*), chosen based on their  
339 relative expression profile in fruit at 49 and 126 DAFB (Tadiello et al., 2016). For  
340 instance, *PpACS1* is dramatically induced by ripening (Trainotti et al., 2007), and  
341 *PpACS2* expression is relatively abundant in fully developed leaves, but it is very low in  
342 fruit, with a peak at the beginning of development (40 DAFB) and a maximum in  
343 senescence (120 DAFB) (Tadiello et al., 2016). As regards to *ACOs*, *PpACO1*  
344 expression is induced by ethylene, *PpACO2* expression is almost constitutive, whereas  
345 *PpACO3* is the less expressed but with a maximum at 115 DAFB (Ruperti et al., 2001;  
346 Tadiello et al., 2016).

347 In the present study, at 49 DAFB, the *ACS* family was expressed at different levels  
348 depending on the strain inoculated and time condition (Fig. 3). As a role, the amount of  
349 *PpACS1* transcripts increased over time, confirming the role of this gene on the ripening  
350 process (Tatsuki et al., 2006), or at least its tight correlation with the fruit ethylene  
351 production. Significant differences among treatments were found at 6 and 8 dpi. At 24

352 hpi, expression levels of *PpACS1* rose up 28-fold, 1,348-fold, 119-fold and 1,188-fold  
353 for CK, CPML11, ML8L and CPMC6, respectively (Fig. 3A). Regarding *PpACS2*,  
354 results showed two distinct expression profiles (Fig. 3B). *PpACS2* has been described to  
355 be induced by abiotic stressors such as wounding (Tatsuki et al., 2006), and negatively  
356 regulated by ethylene in citrus (Marcos et al., 2005). Our results showed a positive  
357 ethylene regulation and hence are not in accordance with data from Marcos et al.  
358 (2005), most likely because we are working on a typical climacteric specie while they  
359 did in a non-climacteric fruit such as citrus. In fact, results from the present study  
360 showed that expression levels of *PpACS2* for both CK and ML8L treatments were very  
361 low and only slightly induced (1.4-fold and 1.6-fold, respectively) at 6 dpi. However,  
362 for the fruit infected with CPML11, an enhanced production at 8 dpi which correlated  
363 with the increased ethylene production was observed. Our results also shown that both  
364 *PpACS1* and *PpACS2* were over-expressed during pathogen-induced senescence.  
365 Enhanced ethylene production is frequently observed during plant–pathogen  
366 interactions, acting as a signalling molecule in response to biotic attacks and hence,  
367 contributing to the induction of the plant response. Such recognition by the plant  
368 immune system elicit host defences, resulting in rapid responses that are triggered by  
369 pathogen-associated molecular patterns (PAMPs) (Jones and Dangl, 2006). Hence, to  
370 establish proliferation, fungi must avoid eliciting PAMP-triggered immunity (PTI) first  
371 line of defence reactions, or either cope with or suppress it. Another measure for  
372 controlling the defences of the whole plant against infections by pathogens is through  
373 the systemic acquired resistance (SAR) in which ethylene has also been implicated  
374 (Ryals et al., 1996). In agreement to the above mentioned, the fact that these defence  
375 mechanisms might been activated after the onset of brown rot symptoms reinforce the  
376 hypothesis of the suppression of the natural ethylene production pattern as a strategy of

377 the fungus to inhibit SAR, jasmonic acid signalling cascades and thereby phenylalanine  
378 ammonia-lyase (PAL) biosynthesis, and hence facilitate colonisation.

379 As refers to the *ACO* family at 49 DAFB, a complex expression pattern was obtained,  
380 and remarkably, expression levels of *PpACO1* were considerably higher than those of  
381 both *PpACO2* and *PpACO3* (Fig. 4), in agreement with the studies already published  
382 (Tadiello et al., 2016). For *PpACO1* significant differences were found depending on  
383 the strain inoculated (Fig. 4A). In detail, at 72 hpi it was detected a transient increase up  
384 to 230-fold, 101-fold and 135.5-fold for CPMC6, CPML11 and ML8L, respectively. At  
385 6 dpi, a decrease was monitored in all the treatments, except for the control that reached  
386 its maximum expression level (190-fold). The results obtained for the control were in  
387 agreement with previous studies (Tonutti et al., 1997), which demonstrate an increase in  
388 ethylene production enhanced by the up-regulation of *PpACO1*. At 8 dpi, the expression  
389 profile was the opposite; while the levels of the control fruit decreased with respect to 6  
390 dpi, the infected fruit experienced and up-regulation of *PpACO1* levels irrespective of  
391 the fungus, and this could be likely related to senescence. As observed for *PpACO1*, an  
392 up-regulation at 6 dpi was also obtained for *PpACO2* for the CK sample, coinciding  
393 with the maximum ethylene production. However, levels were very low if compared to  
394 *PpACO1* and are somehow confirming that this isogene is not strictly involved with the  
395 climacteric system II (Tadiello et al., 2010). Regarding *PpACO3*, a tendency to the up-  
396 regulation was observed at 24 hpi for both CPML11 and CPMC6, being in line with  
397 *PpACO2* at 24 hpi. These findings also coincide with the ones observed in apple-*P.*  
398 *expansum* interaction, in which a massive induction of *MdACO3* expression was  
399 observed after the inoculation with the compatible pathogen (Vilanova et al., 2017). In  
400 other climacteric fruits such as apple *ACO* has been related in the transition from  
401 system I to system II, being negatively regulated by ethylene (Bulens et al., 2014),

402 which correlates with the results presented herein since the peaks of ethylene production  
403 took place when expression levels of this transcript were reduced. The strain ML8L  
404 triggered an induction of this gene but only at 8 dpi (4-fold) (Fig. 4C). Overall, our  
405 results suggest that the inhibition of the fruit ethylene production by the *Monilinia* spp.  
406 short after inoculation was not strictly regulated at the molecular level of the ethylene  
407 biosynthetic pathway. It is therefore likely that other mechanisms are used by the fungi  
408 at this developmental stage to inhibit the ethylene burst occurred and hence suppress  
409 SAR. In other fruit-pathosystems, polyamines have been shown to play a pivotal role in  
410 determining the fruit susceptibility to pathogen infection (Nambeesan et al., 2012).  
411 Accordingly, it is acknowledged that biosynthesis of both polyamines and ethylene  
412 share *S*-AdoMet as a common precursor (Pandey et al., 2000). In fact, peach fruit  
413 treated with polyamines putrescine and spermidine has demonstrated to inhibit ethylene  
414 production, interfering at both biochemical and molecular level (Ziosi et al., 2006).  
415 Besides, transgenic tomato lines overexpressing an enzyme involved in polyamine  
416 biosynthesis were more susceptible to *B. cinerea* (Nambeesan et al., 2012). Thus, during  
417 *Monilinia* infection, enhanced secretion of fungi polyamines may explain the down-  
418 regulation of genes involved in ethylene biosynthesis, which in turn could also lowered  
419 the defence responses resulting in higher brown rot incidence. Furthermore, the  
420 suppression of ethylene observed at 49 DAFB, but not at 126 DAFB, is in line with  
421 Apelbaum et al. (1981), who reported that polyamines are more effective in inhibiting  
422 ethylene at earlier fruit developmental stages. Another explanation may relate to fungal  
423 secretion of effectors that suppress the host immune response or manipulate host cell  
424 physiology (reviewed in Lo Presti et al., 2015). Nonetheless, further studies are warrant  
425 to decipher the mode of action for *Monilinia* spp. to infect stone fruit at earlier  
426 developmental stages.

427 Analogous to what occurred at 49 DAFB for ACS family, at 126 DAFB, expression  
428 levels were larger than those observed for the ACO family. Notably, both *PpACS1* (Fig.  
429 5A) and *PpACS2* (Fig. 5B) followed the same pattern and precede or parallel the  
430 ethylene peak, demonstrating a positive ethylene regulation. Besides, significant  
431 differences were found depending on the strain inoculated, especially at 6 dpi (Fig. 5).  
432 At this sampling point, CPMC6 induced the largest expression (767-fold) for *PpACS1*,  
433 followed by CPML11 (330-fold), and ML8L (25-fold) and CK (2-fold) (Fig. 5A).  
434 Again, the increased expression levels coincided with the major ethylene production,  
435 confirming the positive role of this gene on the ethylene biosynthesis and pointing out  
436 the capacity of these fungi to alter gene expression to ultimately induce ethylene  
437 production. By the moment, no data regarding ethylene production by *Monilinia* has  
438 been described and preliminary results pointed out that this fungus is not able to  
439 produce ethylene by itself unless grown in very specific conditions (unpublished data).  
440 Hence, it is feasible to attribute the higher ethylene production to the up-regulation of  
441 *PpACS1*. At this phenological stage, it seems that increased ethylene production is not  
442 parallel by an action of SAR, or at least that the three strains, and especially CPMC6  
443 and CPML11, were likely capable of coping with it and hence benefit from it. For  
444 instance, the increased ethylene synthesis due to *PpACS1* induction may lead to the  
445 autocatalytic ethylene evolution characteristic of system 2 ethylene (Mathooko et al.,  
446 2001; Tatsuki et al., 2006), which, in turn, could trigger polygalacturonase (PG) and  
447 pectin methyl esterase (PME) actions (Hayama et al., 2006). It is known that both  
448 enzymes contribute to the weakening of peach tissue following cell wall degradation  
449 (Brummell et al., 2004), and thus their action could facilitate penetration. For *PpACS2*,  
450 CPML11 induced the highest expression levels at 24 hpi (4.2-fold) and 6 dpi (709-fold),  
451 while no significant differences were found among CPMC6, ML8L and CK (Fig. 5B).

452 In the control fruit, and as described before for this development stage (Tadiello et al.,  
453 2016), very low levels were detected during the time course of the experiment. Taking  
454 all together, these results demonstrate the capability of *Monilinia* spp. to alter the  
455 expression of genes related to ethylene biosynthesis and, consequently, ethylene  
456 production before initiation of decay.

457 In contrast to that described above, *ACO* family was poorly expressed (Fig. 6),  
458 especially if compared to 49 DAFB. This trend is likely related to the fact that at this  
459 phenological stage we did not observed ethylene production in the control fruit. Hence,  
460 the expression levels of *PpACO* were very low and in line with the lower ethylene  
461 capacity of the non-inoculated fruit. Briefly, for *PpACO1* significant differences were  
462 found between strains CPML11 and ML8L at 72 and 6 dpi (Fig. 6A), displaying the  
463 different capability of this two strains to modulate the expression of this gene. For  
464 *PpACO2* significant differences among strains were only found at 6 dpi, when CPML11  
465 enhanced the induction of the transcript levels of this gene by 3.4-fold (Fig. 6B). At the  
466 other time points, none of the infected samples changed significantly the expression  
467 levels of this transcript, being almost constitutive as reported earlier (Tadiello et al.,  
468 2016). On the other hand, for *PpACO3* significant differences were found earlier,  
469 especially at 24 hpi, when a significant increase of 2.6-fold was monitored for CPML11  
470 (Fig. 6C). This up-regulation concurred with the moment when ethylene levels were  
471 almost null, which correlates with its implication with system I reported in previous  
472 works (Vilanova et al., 2017). In general, the low expression levels in this family could  
473 explain the nearly constant ethylene production pattern observed in the control fruit at  
474 this development stage compared to 49 DAFB, although no increase in genes involved  
475 in system I, such as *PpACO3* is demonstrated. Moreover, these findings explain that the

476 increase in ethylene production of the infected fruit, at least, is not the result of *PpACO3*  
477 alteration.

#### 478 **4. Conclusions**

479 Collectively, it could be observed that the strains of *Monilinia*, through different  
480 mechanisms that depend on the fruit developmental stage, succeed in infecting peaches.  
481 At 49 DAFB, in which we have demonstrated a climacteric-like behaviour, the infected  
482 fruit failed to display normal defence reactions, which included ethylene synthesis and  
483 increased respiration until, at least, 6 dpi, when a clear development of the decay was  
484 already observed. Besides, such inhibition of the ethylene production by *Monilinia* spp.  
485 to avoid SAR responses and facilitate colonisation was not mediated at the molecular  
486 level, pointing out that other pathways, including the production of polyamines, could  
487 have been implicated. On the other hand, at 126 DAFB ethylene production precede the  
488 symptoms of decay development, likely enhancing the capability of *Monilinia* spp. to  
489 successfully infect stone fruit through the putative activation of pectin-degrading enzymes  
490 that accelerate the rate of softening. Finally, by looking at the control for both  
491 phenological stages, we have demonstrated that *PpACSI* is the key gene involved in the  
492 ethylene biosynthetic pathway, and at 126 DAFB, in which a non-climacteric behaviour  
493 was observed, also a suitable target that *Monilinia* spp. tend to up-regulate to induce  
494 changes associated with increasing susceptibility to infection. Such knowledge is  
495 critical for understanding the host (peach) and the pathogen (*Monilinia* spp.) factors  
496 important for the rapid spread and dramatic impact of brown rot and may open new  
497 paths for the control of this disease.

#### 498 **5. Contributions**

499 JGB, NBM and RT conceived and designed the experiment. NBM, NV and JGB  
500 analysed all the data. NBM, JGB and NV were responsible for the ethylene and  
501 respiration rate measurements. NBM, NV and SS were responsible for the gene  
502 expression analysis. NT and JU led the fruit inoculation and pathogenicity studies.  
503 NBM, NV, JGB and RT wrote the article and all remaining authors contributed in  
504 improving the final version of the manuscript.

## 505 **6. Acknowledgements**

506 Authors are grateful to the Spanish Government for their financial support by national  
507 projects AGL2014-55287-C02-02-R and AGL2017-84389-C2-1-R from Ministry of  
508 Economy, Industry and Competitiveness (MINECO), to the Catalan Government  
509 (Generalitat de Catalunya) for the PhD grant 2018FI\_B2\_00184 (Baró-Montel, N.) and for  
510 the funding received from CERCA Programme / Generalitat de Catalunya. The authors  
511 would also like to thank Violeta Lindo for her technical assistance with ethylene  
512 measurements. All authors declare that they have no conflicts of interest in relation to  
513 this publication.

## 514 **References**

515 Apelbaum, A., Burgoon, A.C., Anderson, J.D., Lieberman, M., Ben-Arie, R., Mattoo,  
516 A.K., 1981. Polyamines inhibit biosynthesis of ethylene in higher plant tissue and  
517 fruit protoplasts. *Plant Physiol.* 68, 453–456. <https://doi.org/10.1104/pp.68.2.453>  
518 Argueso, C.T., Hansen, M., Kieber, J.J., 2007. Regulation of ethylene biosynthesis. *J.*  
519 *Plant Growth Regul.* 26, 92–105.  
520 Ballester, A.R., Lafuente, M.T., Forment, J., Gadea, J., de Vos, R.C.H., Bovy, A.G.,  
521 González-Candelas, L., 2011. Transcriptomic profiling of citrus fruit peel tissues  
522 reveals fundamental effects of phenylpropanoids and ethylene on induced



- 523 resistance. *Mol. Plant Pathol.* 12, 879–897. <https://doi.org/10.1111/j.1364->  
524 3703.2011.00721.x
- 525 Ballester, A.R., Lafuente, M.T., González-Candelas, L., 2006. Spatial study of  
526 antioxidant enzymes, peroxidase and phenylalanine ammonia-lyase in the citrus  
527 fruit-*Penicillium digitatum* interaction. *Postharvest Biol. Technol.* 39, 115–124.  
528 <https://doi.org/10.1016/j.postharvbio.2005.10.002>
- 529 Basset, C.L., Artlip, T.S., Callahan, A.M., 2002. Characterization of the peach  
530 homologue of the ethylene receptor, *PpETR1*, reveals some unusual features  
531 regarding transcript processing. *Planta* 215, 679–688.
- 532 Blanco-Ulate, B., Vincenti, E., Powell, A.L.T., Cantu, D., 2013. Tomato transcriptome  
533 and mutant analyses suggest a role for plant stress hormones in the interaction  
534 between fruit and *Botrytis cinerea*. *Front. Plant Sci.* 4, 1–16.  
535 <https://doi.org/10.3389/fpls.2013.00142>
- 536 Bleecker, A.B., Kende, H., 2000. Ethylene: a gaseous signal molecule in plants. *Annu.*  
537 *Rev. Cell Dev. Biol.* 16, 1–18.
- 538 Broekgaarden, C., Caarls, L., Vos, I.A., Pieterse, C.M.J., Wees, S.C.M. Van, 2015.  
539 Ethylene: a traffic controller on hormonal crossroads to defense. *Plant Physiol.*  
540 169, 2371–2379.
- 541 Brummell, D.A., Dal Cin, V., Crisosto, C.H., Labavitch, J.M., 2004. Cell wall  
542 metabolism during maturation, ripening and senescence of peach fruit. *J. Exp. Bot.*  
543 55, 2029–2039. <https://doi.org/10.1093/jxb/erh227>
- 544 Bulens, I., Van de Poel, B., Hertog, M.L.A.T.M., Cristescu, S.M., Harren, F.J.M., De  
545 Proft, M.P., Geeraerd, A.H., Nicolai, B.M., 2014. Dynamic changes of the ethylene  
546 biosynthesis in ‘Jonagold’ apple. *Physiol. Plant.* 150, 161–173.  
547 <https://doi.org/10.1111/ppl.12084>

- 548 De Vos, M., Van Oosten, V.R., Van Poecke, R.M.P., Van Pelt, J.A., Pozo, M.J.,  
549 Mueller, M.J., Buchala, A.J., Métraux, J.-P., Van Loon, L.C., Dicke, M., Pieterse,  
550 C.M.J., 2005. Signal signature and transcriptome changes of *Arabidopsis* during  
551 pathogen and insect attack. *Mol. Plant-Microbe Interact.* 18, 923–937.  
552 <https://doi.org/10.1094/MPMI-18-0923>
- 553 Di, X., Gomila, J., Takken, F.L.W., 2017. Involvement of salicylic acid, ethylene and  
554 jasmonic acid signalling pathways in the susceptibility of tomato to *Fusarium*  
555 *oxysporum*. *Mol. Plant Pathol.* 18, 1024–1035. <https://doi.org/10.1111/mpp.12559>
- 556 Ecker, J.R., Davis, R.W., 1987. Plant defense genes are regulated by ethylene. *Proc.*  
557 *Natl. Acad. Sci. U. S. A.* 84, 5202–5206. <https://doi.org/10.1073/pnas.84.15.5202>
- 558 Giné-Bordonaba, J., Echeverria, G., Ubach, D., Aguiló-Aguayo, I., López, M.L.,  
559 Larrigaudière, C., 2017. Biochemical and physiological changes during fruit  
560 development and ripening of two sweet cherry varieties with different levels of  
561 cracking tolerance. *Plant Physiol. Biochem.* 111, 216–225.  
562 <https://doi.org/10.1016/j.plaphy.2016.12.002>
- 563 Glazebrook, J., 2005. Contrasting mechanisms of defense against biotrophic and  
564 necrotrophic pathogens. *Annu. Rev. Phytopathol.* 43, 205–225.  
565 <https://doi.org/10.3109/9781841847481>
- 566 Guidarelli, M., Zubini, P., Nanni, V., Bonghi, C., Rasori, A., Bertolini, P., Baraldi, E.,  
567 2014. Gene expression analysis of peach fruit at different growth stages and with  
568 different susceptibility to *Monilinia laxa*. *Eur. J. Plant Pathol.* 140, 503–513.  
569 <https://doi.org/https://doi.org/10.1007/s10658-014-0484-8>
- 570 Hall, R., 1967. Effect of *Monilinia fructicola* on oxygen uptake of peach fruits. *J.*  
571 *Phytopathol.* 58, 131–136.
- 572 Hayama, H., Shimada, T., Fujii, H., Ito, A., Kashimura, Y., 2006. Ethylene-regulation

- 573 of fruit softening and softening-related genes in peach. *J. Exp. Bot.* 57, 4071–4077.
- 574 Jones, J.D.G., Dangl, J.L., 2006. The plant immune system. *Nature* 444, 323–329.
- 575 <https://doi.org/10.1038/nature05286>
- 576 Landi, L., De Miccolis Angelini, R., Pollastro, S., Abate, D., Faretra, F., Romanazzi, G.,
- 577 2018. Genome sequence of the brown rot fungal pathogen *Monilinia fructigena*.
- 578 *BMC Res. Notes* 11, 10–12. <https://doi.org/10.1186/s13104-018-3854-z>
- 579 Lo Presti, L., Lanver, D., Schweizer, G., Tanaka, S., Liang, L., Tollot, M., Zuccaro, A.,
- 580 Reissmann, S., Kahmann, R., 2015. Fungal effectors and plant susceptibility.
- 581 *Annu. Rev. Plant Biol.* 66, 513–545. [https://doi.org/10.1146/annurev-arplant-](https://doi.org/10.1146/annurev-arplant-043014-114623)
- 582 [043014-114623](https://doi.org/10.1146/annurev-arplant-043014-114623)
- 583 Marcos, J.F., González-Candelas, L., Zacarías, L., 2005. Involvement of ethylene
- 584 biosynthesis and perception in the susceptibility of citrus fruits to *Penicillium*
- 585 *digitatum* infection and the accumulation of defence-related mRNAs. *J. Exp. Bot.*
- 586 56, 2183–2193. <https://doi.org/10.1093/jxb/eri218>
- 587 Mathooko, F.M., Tsunashima, Y., Owino, W.Z.O., Kubo, Y., Inaba, A., 2001.
- 588 Regulation of genes encoding ethylene biosynthetic enzymes in peach (*Prunus*
- 589 *persica* L.) fruit by carbon dioxide and 1-methylcyclopropene. *Postharvest Biol.*
- 590 *Technol.* 21, 265–281. [https://doi.org/10.1016/S0925-5214\(00\)00158-7](https://doi.org/10.1016/S0925-5214(00)00158-7)
- 591 Nambeesan, S., AbuQamar, S., Laluk, K., Mattoo, A.K., Mickelbart, M. V., Ferruzzi,
- 592 M.G., Mengiste, T., Handa, A.K., 2012. Polyamines attenuate ethylene-mediated
- 593 defense responses to abrogate resistance to *Botrytis cinerea* in tomato. *Plant*
- 594 *Physiol.* 158, 1034–1045. <https://doi.org/10.1104/pp.111.188698>
- 595 Naranjo-Ortíz, M.A., Rodríguez-Pires, S., Torres, R., De Cal, A., Usall, J., Gabaldón,
- 596 T., 2018. Genome sequence of the brown rot fungal pathogen *Monilinia laxa*.
- 597 *Genome Announc.* 6, 10–12. <https://doi.org/10.1128/genomeA.00214-18>

- 598 Pandey, D., Rajendran, S.R.C.K., Gaur, M., Sajeesh, P.K., Kumar, A., 2016. Plant  
599 defense signaling and responses against necrotrophic fungal pathogens. *J. Plant*  
600 *Growth Regul.* 35, 1159–1174. <https://doi.org/10.1007/s00344-016-9600-7>
- 601 Pandey, S., Ranade, S.A., Nagar, P.K., Kumar, N., 2000. Role of polyamines and  
602 ethylene as modulators of plant senescence. *J. Biosci.* 25, 291–299.  
603 <https://doi.org/10.1007/BF02703938>
- 604 Payton, S., Fray, R.G., Brown, S., Grierson, D., 1996. Ethylene receptor expression is  
605 regulated during fruit ripening, flower senescence and abscission. *Plant Mol. Biol.*  
606 31, 1227–1231.
- 607 Pétriacq, P., López, A., Luna, E., 2018. Fruit decay to diseases: can induced resistance  
608 and priming help? *Plants* 7, 1–16.  
609 <https://doi.org/https://doi.org/10.3390/plants7040077>
- 610 Pfaffl, M.W., 2001. A new mathematical model for relative quantification in real-time  
611 RT-PCR. *Nucleic Acids Res.* 29, 16–21. <https://doi.org/10.1093/nar/29.9.e45>
- 612 Rasori, A., Ruperti, B., Bonghi, C., Tonutti, P., Ramina, A., 2002. Characterization of  
613 two putative ethylene receptor genes expressed during peach fruit development and  
614 abscission. *J. Exp. Bot.* 53, 2333–2339.
- 615 Rivera, Y., Zeller, K., Srivastava, S., Sutherland, J., Galvez, M., Nakhla, M.,  
616 Poniatowska, A., Schnabel, G., Sundin, G., Abad, Z.G., 2018. Draft genome  
617 resources for the phytopathogenic fungi *Monilinia fructicola*, *M. fructigena*, *M.*  
618 *polystroma*, and *M. laxa*, the causal agents of brown rot. *Phytopathology* 108,  
619 1141–1142.
- 620 Ruperti, B., Bonghi, C., Rasori, A., Ramina, A., Tonutti, P., 2001. Characterization and  
621 expression of two members of the peach 1-aminocyclopropane-1-carboxylate  
622 oxidase gene family. *Physiol. Plant.* 111, 336–344. <https://doi.org/10.1034/j.1399->

- 623 3054.2001.1110311.x
- 624 Ryals, J.A., Neuenschwander, U.H., Willits, M.G., Molina, A., Steiner, H.-Y., Hunt,  
625 M.D., 1996. Systemic Acquired Resistance. *Plant Cell* 8, 1809–1819.  
626 <https://doi.org/https://doi.org/10.1105/tpc.8.10.1809>
- 627 Tadiello, A., Trainotti, L., Ziosi, V., Costa, G., 2010. Genes involved in the control of  
628 ethylene biosynthesis during climacteric of *Prunus persica* fruit. *Acta Hortic.* 67–  
629 72. <https://doi.org/10.17660/ActaHortic.2010.884.5>
- 630 Tadiello, A., Ziosi, V., Negri, A.S., Noferini, M., Fiori, G., Busatto, N., Trainotti, L.,  
631 2016. On the role of ethylene, auxin and a GOLVEN-like peptide hormone in the  
632 regulation of peach ripening. *BMC Plant Biol.* 16, 1–17.
- 633 Tatsuki, M., Haji, T., Yamaguchi, M., 2006. The involvement of 1-aminocyclopropane-  
634 1-carboxylic acid synthase isogene, *Pp-ACS1*, in peach fruit softening. *J. Exp. Bot.*  
635 57, 1281–1289. <https://doi.org/10.1093/jxb/erj097>
- 636 Thynne, E., McDonald, M.C., Solomon, P.S., 2015. Phytopathogen emergence in the  
637 genomic era. *Trends Plant Sci.* 20, 246–255.
- 638 Tian, S., Torres, R., Ballester, A.R., Li, B., Vilanova, L., González-Candelas, L., 2016.  
639 Molecular aspects in pathogen-fruit interactions: Virulence and resistance.  
640 *Postharvest Biol. Technol.* 122, 11-21  
641 <https://doi.org/10.1016/j.postharvbio.2016.04.018>
- 642 Tong, Z., Gao, Z., Wang, F., Zhou, J., Zhang, Z., 2009. Selection of reliable reference  
643 genes for gene expression studies in peach using real-time PCR. *BMC Mol. Biol.*  
644 10, 1–13. <https://doi.org/10.1186/1471-2199-10-71>
- 645 Tonutti, P., Bonghi, C., ... B.R.-J. of the, 1997, U., 1997. Ethylene evolution and 1-  
646 aminocyclopropane-1-carboxylate oxidase gene expression during early  
647 development and ripening of peach fruit. *J. Am. Soc. Hortic. Sci.* 122, 642–647.

- 648 Trainotti, L., Tadiello, A., Casadoro, G., 2007. The involvement of auxin in the ripening  
649 of climacteric fruits comes of age: the hormone plays a role of its own and has an  
650 intense interplay with ethylene in ripening peaches. *J. Exp. Bot.* 58, 3299–3308.  
651 <https://doi.org/10.1093/jxb/erm178>
- 652 van Loon, L.C., Geraats, B.P.J., Linthorst, H.J.M., 2006. Ethylene as a modulator of  
653 disease resistance in plants. *Trends Plant Sci.* 11, 184–191.  
654 <https://doi.org/10.1016/j.tplants.2006.02.005>
- 655 Verde, I., Abbott, A.G., Scalabrin, S., Jung, S., Shu, S., Marroni, F., Zhebentyayeva, T.,  
656 Dettori, M.T., Grimwood, J., Cattonaro, F., Zuccolo, A., Rossini, L., Jenkins, J.,  
657 Vendramin, E., Meisel, L.A., Decroocq, V., Sosinski, B., Prochnik, S., Mitros, T.,  
658 Policriti, A., Cipriani, G., Dondini, L., Ficklin, S., Goodstein, D.M., Xuan, P., Del  
659 Fabbro, C., Aramini, V., Copetti, D., Gonzalez, S., Horner, D.S., Falchi, R., Lucas,  
660 S., Mica, E., Maldonado, J., Lazzari, B., Bielenberg, D., Pirona, R., Miculan, M.,  
661 Barakat, A., Testolin, R., Stella, A., Tartarini, S., Tonutti, P., Arús, P., Orellana,  
662 A., Wells, C., Main, D., Vizzotto, G., Silva, H., Salamini, F., Schmutz, J.,  
663 Morgante, M., Rokhsar, D.S., 2013. The high-quality draft genome of peach  
664 (*Prunus persica*) identifies unique patterns of genetic diversity, domestication and  
665 genome evolution. *Nat. Genet.* 45, 487–494. <https://doi.org/10.1038/ng.2586>
- 666 Vilanova, L., Vall-Illaura, N., Torres, R., Usall, J., Teixidó, N., Larrigaudière, C., Giné-  
667 Bordonaba, J., 2017. *Penicillium expansum* (compatible) and *Penicillium digitatum*  
668 (non-host) pathogen infection differentially alter ethylene biosynthesis in apple  
669 fruit. *Plant Physiol. Biochem.* 120, 132–143.  
670 <https://doi.org/10.1016/j.plaphy.2017.09.024>
- 671 Wang, K.-C., Li, H., Ecker, J., 2002. Ethylene biosynthesis and signaling networks.  
672 *Plant Cell* 14, 31–51.

- 673 Wang, X., Ding, Y., Wang, Y., Pan, L., Niu, L., Lu, Z., Cui, G., Zeng, W., Wang, Z.,  
674 2017. Genes involved in ethylene signal transduction in peach (*Prunus persica*)  
675 and their expression profiles during fruit maturation. *Sci. Hortic.* (Amsterdam).  
676 224, 306–316. <https://doi.org/10.1016/j.scienta.2017.06.035>
- 677 Yang, S.F., Hoffmann, N.E., 1984. Ethylene biosynthesis and its regulation in higher  
678 plants. *Annu. Rev. Plant Physiol.* 35, 155–189.
- 679 Zhao, S., Hong, W., Wu, J., Wang, Y., Ji, S., Zhu, S., Wei, C., Zhang, J., Li, Y., 2017.  
680 A viral protein promotes host SAMS1 activity and ethylene production for the  
681 benefit of virus infection. *Elife* 6. <https://doi.org/10.7554/eLife.27529>
- 682 Zhu, L., Guo, J., Ma, Z., Wang, J., Zhou, C., 2018. *Arabidopsis* transcription factor  
683 MYB102 increases plant susceptibility to aphids by substantial activation of  
684 ethylene biosynthesis. *Biomolecules* 8, 39. <https://doi.org/10.3390/biom8020039>
- 685 Ziosi, V., Bregoli, A.M., Bonghi, C., Fossati, T., Biondi, S., Costa, G., Torrigiani, P.,  
686 2006. Transcription of ethylene perception and biosynthesis genes is altered by  
687 putrescine, spermidine and aminoethoxyvinylglycine (AVG) during ripening in  
688 peach fruit (*Prunus persica*). *New Phytol.* 172, 229–238.  
689 <https://doi.org/10.1111/j.1469-8137.2006.01828.x>
- 690

**Table 1.** Brown rot incidence (%) of ‘Merryl O’Henry’ peach fruit inoculated with different strains of *Monilinia* spp. at 49 and 126 d after full bloom (DAFB). Fruit were inoculated by immersion for 60 s in a conidial suspension containing  $10^5$  conidia mL<sup>-1</sup> of strain CPMC6 of *M. fructicola* (■) or strains CPML11 (■) and ML8L (■) of *M. laxa*, and incubated for 7 d at 20 °C and 100 % relative humidity. Data represent the mean (n = 40) ± S.D. Mean values with the same uppercase letter within the same strain or mean values with the same lowercase letter within the same phenological stage are not significantly different according to analysis of variance (ANOVA) and Tukey’s HSD test ( $p < 0.05$ ).

Phenological stage (DAFB)	Strain		
	CPMC6	CPML11	ML8L
<b>49</b>	100 ± 0.0	100 ± 0.0	40 ± 8.2
<b>126</b>	100 ± 0.0	90 ± 8.2	22.5 ± 12.6





**Fig. 1.** Images of *in vitro* (A) and *in vivo* (B and C) phenotypic differences among three strains of *Monilinia* spp.: *M. fructicola* (CPMC6) and *M. laxa* (ML8L and CPML11). Images A and C were captured 7 d after the fungal inoculation, whereas image B was captured 14 d after the fungal inoculation.

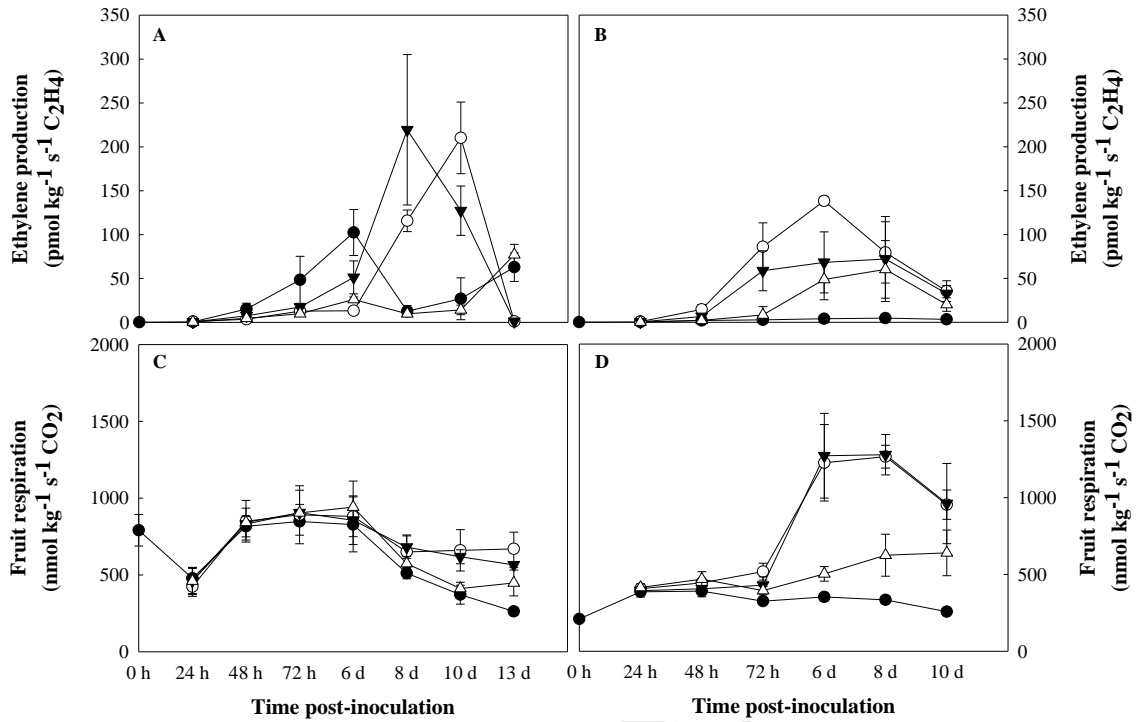


**Fig. 2.** Changes in ethylene production ( $\text{pmol kg}^{-1} \text{s}^{-1} \text{C}_2\text{H}_4$ ) and fruit respiration ( $\text{nmol kg}^{-1} \text{s}^{-1} \text{CO}_2$ ) on a standard fresh weight basis of 'Merryl O'Henry' peach fruit control (●) and inoculated with different strains of *Monilinia* spp. (strain CPMC6 of *M. fructicola* (○) or strains CPML11 (▼) and ML8L (△) of *M. laxa*) at 49 (A and C) and 126 (B and D) d after full bloom (DAFB). Fruit was incubated at 20 °C and 100 % relative humidity until the time of sampling. Each point represents the mean and vertical bars indicate the standard deviation of the mean (n = 4).

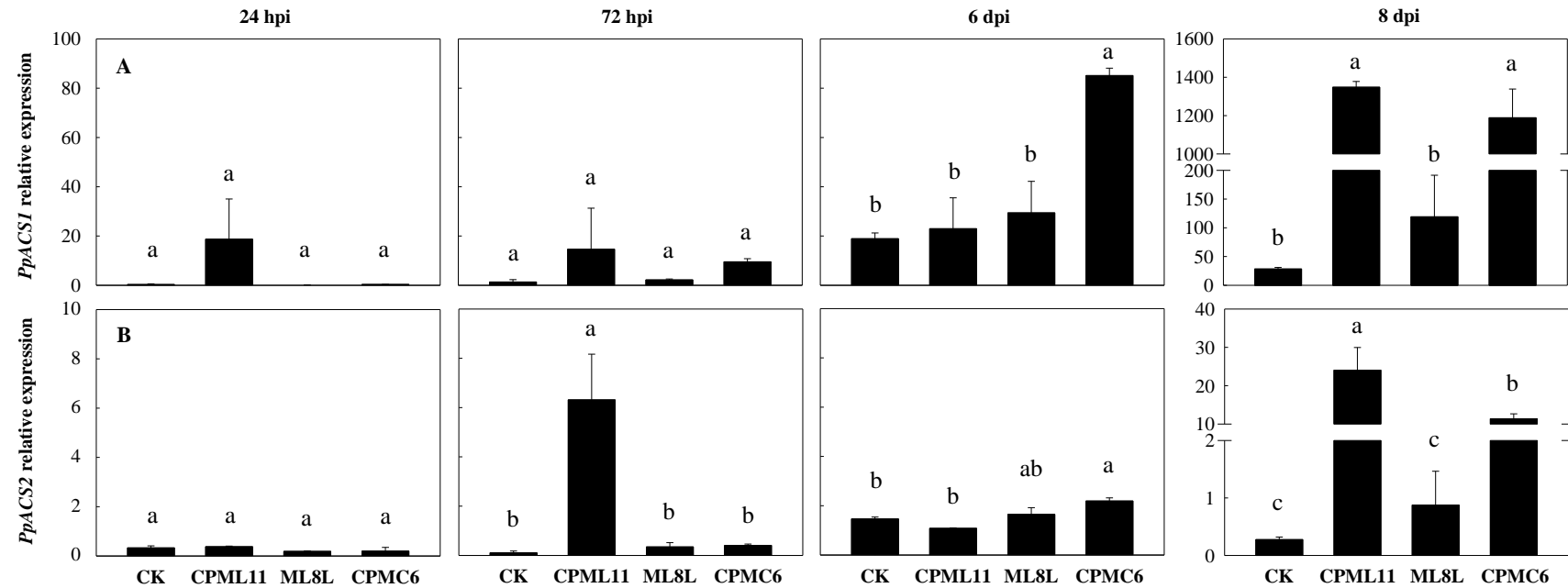


**Fig. 3.** Changes in *in vivo* gene expression levels of *PpACS* family (*PpACS1* (A) and *PpACS2* (B)) of ‘Merryl O’Henry’ peach fruit non-inoculated (CK) and inoculated with strains CPML11 and ML8L of *Monilinia laxa* or CPMC6 of *M. fructicola* at 49 d after full bloom (DAFB). Each column represents the mean of three biological replicates after 24 and 72 hours post-inoculation (hpi), and 6 and 8 d post-inoculation (dpi). At each sampling point, different letters indicate significant differences according to analysis of variance (ANOVA) and Tukey’s HSD test ( $p < 0.05$ ).

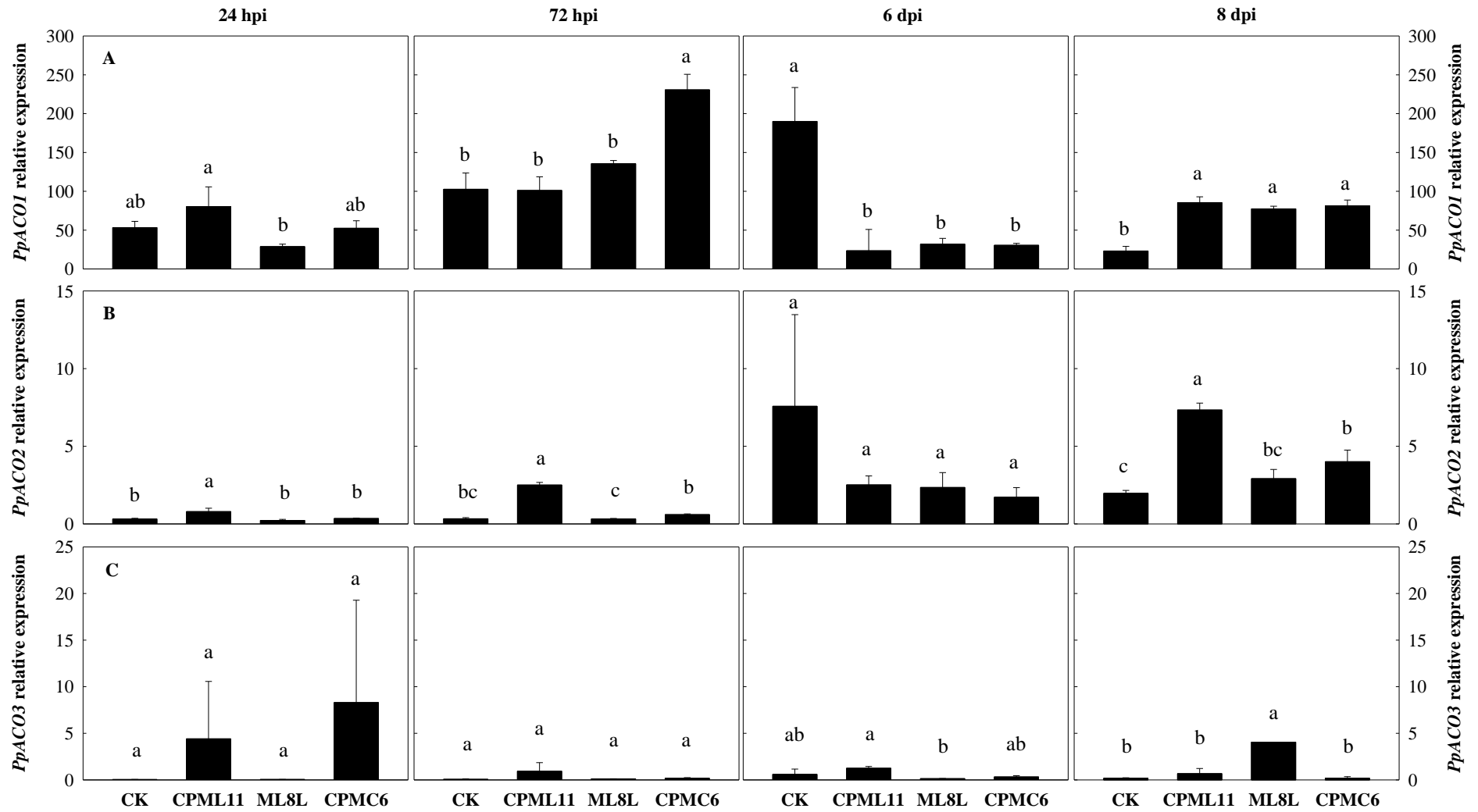


**Fig. 4.** Changes in *in vivo* gene expression levels of *PpACO* family (*PpACO1* (A), *PpACO2* (B) and *PpACO3* (C)) of ‘Merryl O’Henry’ peach fruit non-inoculated (CK) and inoculated with strains CPML11 and ML8L of *Monilinia laxa* or CPMC6 of *M. fructicola* at 49 d after full bloom (DAFB). Each column represents the mean of three biological replicates after 24 and 72 hours post-inoculation (hpi), and 6 and 8 d post-inoculation (dpi). At each sampling point, different letters indicate significant differences according to analysis of variance (ANOVA) and Tukey’s HSD test ( $p < 0.05$ ).

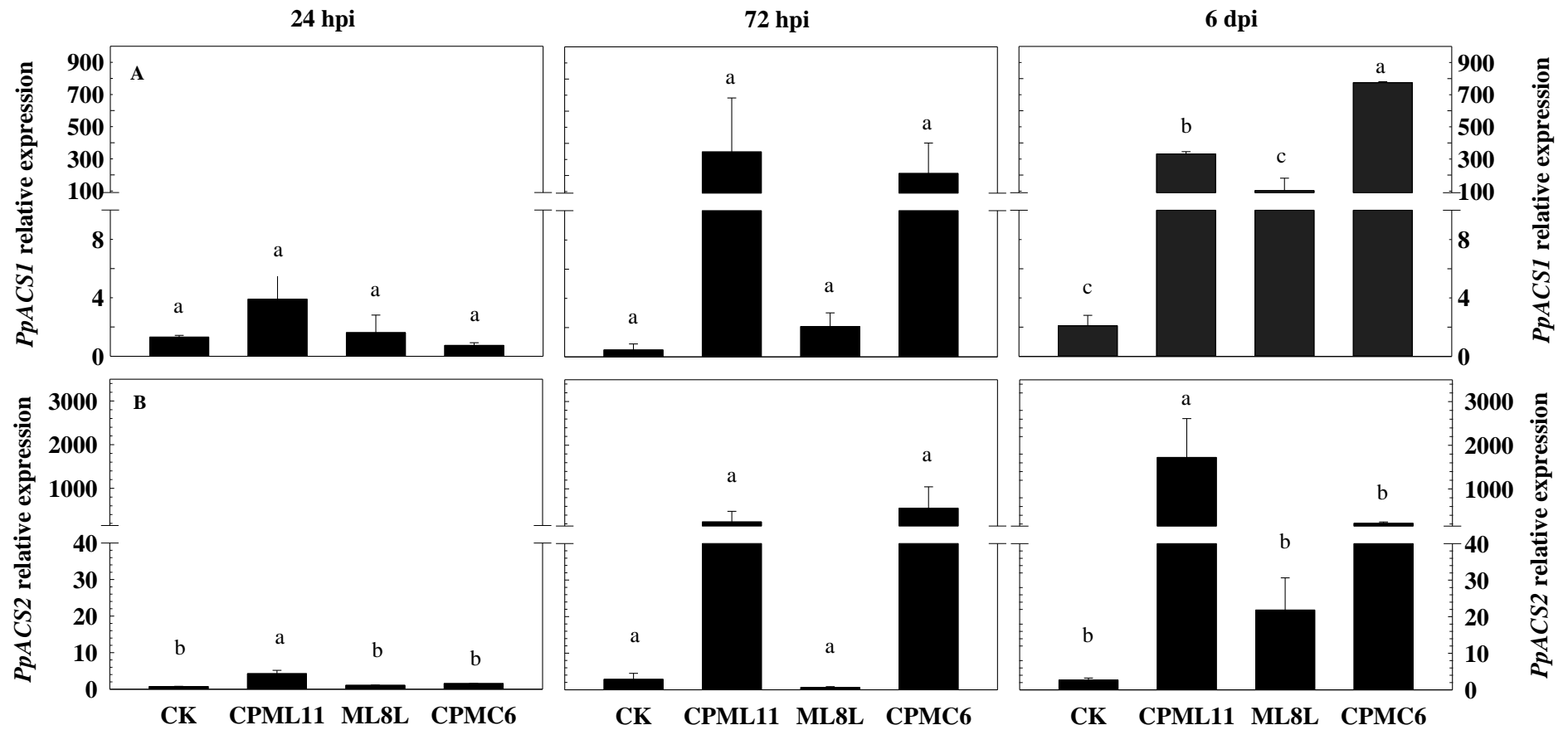


**Fig. 5.** Changes in *in vivo* gene expression levels of *PpACS* family (*PpACS1* (A) and *PpACS2* (B)) of ‘Merryl O’Henry’ peach fruit non-inoculated (CK) and inoculated with strains CPML11 and ML8L of *Monilinia laxa* or CPMC6 of *M. fructicola* at 126 d after full bloom (DAFB).

Each column represents the mean of three biological replicates after 24 and 72 hours post-inoculation (hpi), and 6 d post-inoculation (dpi). At each sampling point, different letters indicate significant differences according to analysis of variance (ANOVA) and Tukey's HSD test ( $p < 0.05$ ).

Journal Pre-proof



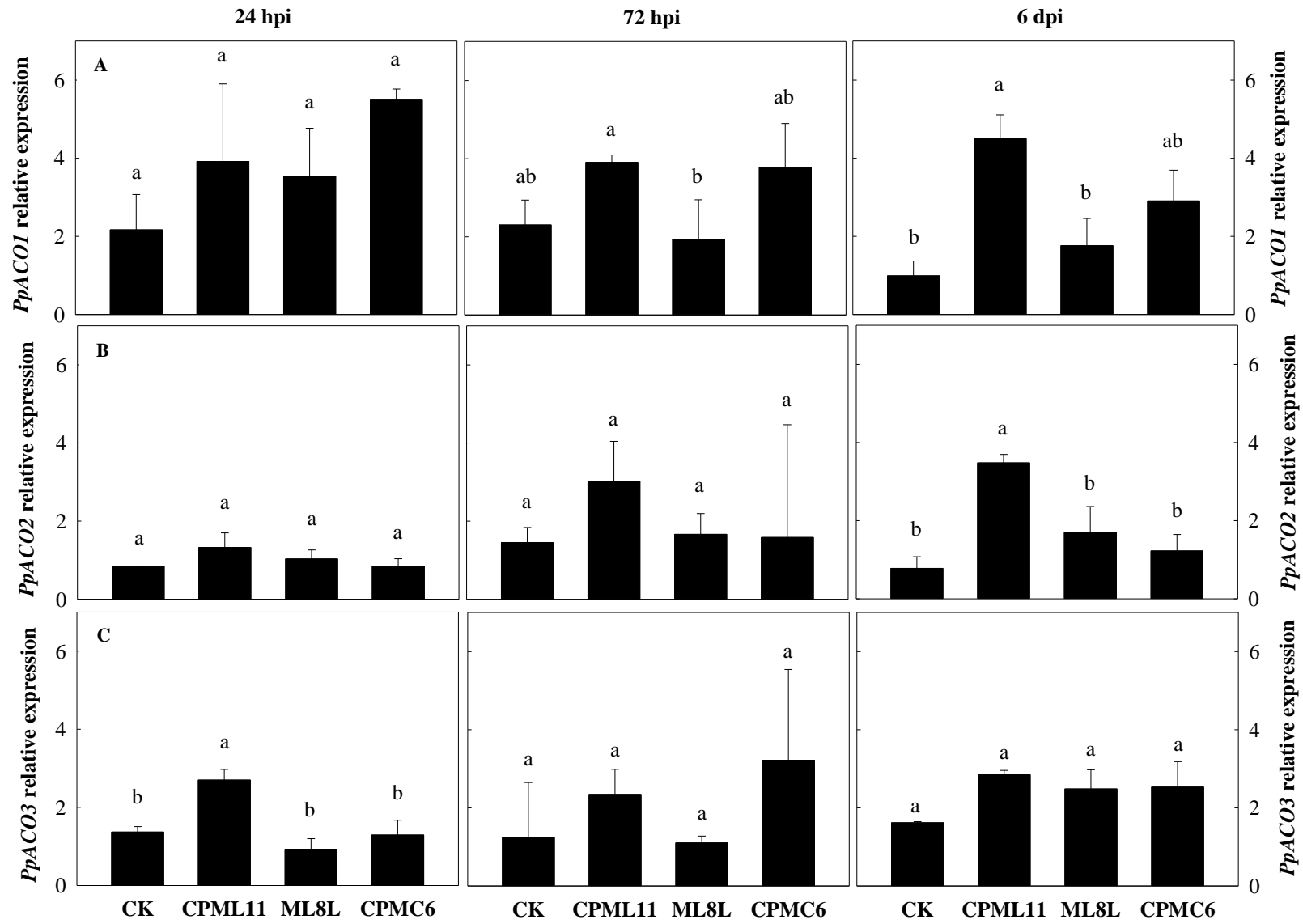


**Fig. 6.** Changes in *in vivo* gene expression levels of *PpACO* family (*PpACO1* (A), *PpACO2* (B) and *PpACO3* (C)) of ‘Merryl O’Henry’ peach fruit non-inoculated (CK) and inoculated with strains CPML11 and ML8L of *Monilinia laxa* or CPMC6 of *M. fructicola* at 126 d after full bloom (DAFB). Each column represents the mean of three biological replicates after 24 and 72 hours post-inoculation (hpi), and 6 d post-inoculation (dpi). At each sampling point, different letters indicate significant differences according to analysis of variance (ANOVA) and Tukey’s HSD test ( $p < 0.05$ ).

**Highlights:**

- Ethylene is a key player with a dual role in determining brown rot susceptibility.
- *Monilinia* infection mechanisms in peach depend on the fruit developmental stage.
- Impairing the ethylene biosynthetic pathway is a putative mechanism by which *Monilinia* spp. is able to infect peach fruit.
- *PpACS1* may be considered as a key gene in the peach-*Monilinia* spp. interactions.

**Author's contributions**

JGB, NBM and RT conceived and designed the experiment. NBM, NV and JGB analysed all the data. NBM, JGB and NV were responsible for the ethylene and respiration rate measurements. NBM, NV and SS were responsible for the gene expression analysis. NT and JU led the fruit inoculation and pathogenicity studies. NBM, NV, JGB and RT wrote the article and all remaining authors contributed in improving the final version of the manuscript.